Journal of Power Sources 195 (2010) 2888–2893

Contents lists available at ScienceDirect

Journal of Power Sources

journal homepage: www.elsevier.com/locate/jpowsour

Short communication

Synthesis and electrochemical properties of multi-doped $LiFePO_4$/C prepared from the steel slag

Z.J. Wu*, H.F. Yue, L.S. Li, B.F. Jiang, X.R. Wu, P. Wang

Anhui Key Laboratory of Metallurgical Engineering & Resources Recycling, Anhui University of Technology, 59 Hudong Road, Maanshan 243002, PR China

ARTICLE INFO

Article history:
Received 23 September 2009
Accepted 13 November 2009
Available online 9 December 2009

Keywords:
Cathode material
$LiFePO_4$
Multi-doping
Steel slag

ABSTRACT

The paper presents and discusses a novel route to synthesize a multi-doped $LiFePO_4$/C composite by using steel slag as a raw material. A ferroalloy with suitable molar ratio of Fe, Mn, V, and Cr is recovered from the slag by a selective carbothermic method, and successfully used as source materials of Fe and multiple dopants for preparing the multi-doped $LiFePO_4$/C. XRD and Rietveld-refined results show that the multi-doped $LiFePO_4$/C is single olivine-type phase and well crystallized, Mn, V, and Cr atoms occupy Fe site. Elemental mapping image confirms that the elements (Fe, P, Mn, V, and Cr) distribute homogeneously in particles of the multi-doped $LiFePO_4$/C. The electrochemical performance of prepared cathode was evaluated by galvanostatic charge/discharge and cyclic voltammogram tests. Compared to the undoped $LiFePO_4$/C prepared only by chemical reagents, the multi-doped $LiFePO_4$/C exhibits lesser capacity drops with increasing of charge/discharge current density due to the improvement of the electrode reactivity by multi-doping. The results suggest that steel slag is an abundant and inexpensive source materials of iron and dopants for preparing multi-doped $LiFePO_4$/C.

1. Introduction

Steel slag with about 10–15 wt.% of the raw steel output is a by-product produced from the steel making. The conventional method for disposal of the slag is dumping. Massive dump of steel slag occupies plenty of land, and has an impact on the environment. Although lots of researches have been devoted to the slag recycling since last 30 years, the effective utilization of the slag is still a problem because of its complex constituents.

The slag contains many valuable elements such as Fe, Mn, P, V and Cr. Previous researches on the slag recycling can be divided into two main categories. One is the direct application of the slag as the metallurgical flux in iron and steel making [1,2]; the other includes recovery of metals from the slag and then application of the tailing in civil engineering projects [3–7] or in soil improvement [8,9]. The metallic iron and Fe-bearing minerals in the slag are recovered by magnetic separation [10] and reused in iron and steel making traditionally, however, the other valuable elements (such as Mn, V, and Cr) within steel slag have been neglected. For the sake of natural resources, it is essential to explore the recovery of the other valuable elements from the slag as well as iron.

The carbothermic method could be used to recover nearly all of Fe in steel slag [11–13]. In fact, many valuable elements (Mn, V, Cr, etc.) in the slag could be recovered along with Fe in the form of ferroalloy by this method. However, the application of such a ferroalloy is a problem owing to the multiple components. Even use as the iron concentrate is limited due to high concentration of phosphorus. It can therefore be concluded that the key to recycling the valuable elements in steel slag is related to two aspects: (1) control on the components of the ferroalloy participated in the slag and (2) a suitable use of the recovered ferroalloy.

Lithium iron phosphate ($LiFePO_4$) is a well-known positive electrode potential candidate for the highpower, safe, low-cost and long-life batteries required to power electric cars. Poor conductivity (either electronic or ionic) is a main obstacle in its commercialization. As a very promising way of improving the intrinsic conductivity of $LiFePO_4$, transition metal ions doping has generated considerable research activity. Among many transition metals, Mn [14–17], V [18,19], and Cr [20–24] doping has been demonstrated beneficial to the electrochemical performance of $LiFePO_4$. It is encouraging that Mn, V, and Cr just consists in steel slag along with plenty of Fe. Thus the slag could be considered an attractive low-cost raw material of multi-doped $LiFePO_4$. The questions are: how to recover the ferroalloy with a suitable concentration of Fe, Mn, V, and Cr from the slag, excluding the unwanted elements in the meantime? Are there what effects of such a source material on the structure and electrochemical properties of the prepared multi-doped $LiFePO_4$?

Trying to answer these questions, the present study introduces and discusses a novel route to synthesize a multi-doped $LiFePO_4$/C (M-$LiFePO_4$/C) by using steel slag as a raw material. The selective carbothermic method was employed to recover the valuable

* Corresponding author. Tel.: +86 555 2311879; fax: +86 555 2311879.
E-mail addresses: wzjof@hotmail.com, wzjof@sina.com (Z.J. Wu).

0378-7753/$ – see front matter © 2009 Elsevier B.V. All rights reserved.
doi:10.1016/j.jpowsour.2009.11.058

Table 1
Average chemical compositions of as-received steel slag and recovered R-oxides.

Compound	Contents (wt.%)	
	As-received steel slag	Recovered R-oxides[a]
TFe	23.26	88.82 (Fe_2O_3)
CaO	49.78	0.08
SiO_2	9.86	0.21
MgO	8.82	0.14
MnO	2.52	4.64
P_2O_5	2.07	3.14
$A1_2O_3$	1.53	0.13
V_2O_5	0.86	1.12
Cr_2O_3	0.53	1.40
TiO_2	0.42	0.02
NiO	0.1	0.04
Residual	0.25	0.26

[a] The recovery ratio of Fe from the slag is about 80 wt.%.

elements from the slag. All of Fe and dopants (Mn, V, and Cr) used for preparing M-$LiFePO_4$/C are provided by the ferroalloy recovered from steel slag in this work. The structure and electrochemical performance of the M-$LiFePO_4$/C prepared from the slag were evaluated and compared with those of undoped $LiFePO_4$/C (U-$LiFePO_4$/C) prepared only by chemical reagents under the same conditions.

2. Experimental

2.1. Recovery of Fe, Mn, V, and Cr from steel slag

The experimental slag used in this study was an industrial steel slag (see Table 1) from a local steel plant. After being crushed by a jaw crusher, the as-received slag was sieved by Tyler Standard Screen. The particles of −10 + 18 mesh were collected for use. The combination of the selective carbothermic process and magnetic separation was used for recovery of the ferroalloy (Fe, Mn, V, and Cr) from the slag. An industrial coke powder with 70 wt.% fixed carbon was used as reductant in the experiment. 200 g of the sieved slag was mixed with the coke powder at a coke/slag ratio of 0.20, and then calcined at 1400 °C for 2.0 h in a crucible furnace under a reductive atmosphere. Then, the sample was slowly cooled down to room temperature in the furnace, and the ferroalloy formed in the slag. The reduced slag was then ground in a ball mill at 500 rpm for 10 h, and the ferroalloy was subsequently separated from tailing by magnetic separation.

2.2. Preparation of multi-component ferric oxides (R-oxides)

The ferroalloy powder recovered from steel slag was roasted at 600 °C for 5 h in air, and then the R-oxides were obtained. The chemical composition of the prepared R-oxides was also listed in Table 1. The R-oxides will be used as the source material of Fe and multi-doping elements of M-$LiFePO_4$/C in this study.

2.3. Synthesis of M-$LiFePO_4$/C and U-$LiFePO_4$/C samples

M-$LiFePO_4$/C and U-$LiFePO_4$/C samples were prepared via a carbothermic reduction route [25]. To synthesize M-$LiFePO_4$/C, the R-oxides, $LiOH{\cdot}H_2O$ (A.R., >96%), and $NH_4H_2PO_4$ (A.R., >99%) was used as starting materials. The mixture of the starting materials taken in the molar ratio of Li:(Fe + Mn + V + Cr):P = 1.02:1.00:1.00 was milled for 4 h in a rotation speed of 350 rpm by using alcohol as a dispersant, and then dried in oven at 80 °C for 24 h in the air. The obtained powder was then mixed with 30 g polypropylene per mole Li^+, and calcined in a tube furnace at 650 °C for 10 h in nitrogen. Then, it was cooled down to room temperature in the furnace, and the M-$LiFePO_4$/C sample was obtained finally. The U-$LiFePO_4$/C sample was also prepared for comparison through the same procedure in addition to substituting Fe_2O_3 (A.R., >99%) for the R-oxides.

2.4. Materials characterization

The chemical composition of the sample was analyzed by X-ray fluorescence (ARL9800XP+, ARL, Swiss). The crystalline phase of the prepared powders was identified by powder X-ray diffraction (D/Max-RA, Rigaku) using Cu Kα radiation. The diffraction data for Rietveld refinement were obtained at 2θ = 15–120°, with a step size of 0.02°. The morphology of the prepared powders was also observed by scanning electron microscopy (JSM-6380LV, JEOL) operating at beam voltages between 20 and 30 kV. Elemental mapping of the particles for the prepared M-$LiFePO_4$ was analyzed by an energy dispersive X-ray spectroscopy (Genesis 2000, JEOL).

2.5. Electrochemical test

The cathode electrodes were prepared with the active materials, acetylene black and polyvinylidene fluoride (PVDF) binder in a weight ratio of 75:15:10. The electrochemical performances were evaluated with a button cell CR2025 assembled with the cathode, a metal lithium foil as both the anode and reference electrode, polypropylene film (Celgard 2300) as the separator and a solution of 1 M LiPF6 in ethylene carbonate (EC) and dimethyl carbonate (DMC) (1:1 in volume) as the electrolyte. All the organic solvents and electrolyte were of battery grade. Cell construction and sealing were carried out in an argon-filled glove box. Galvanostatic cycling was performed between 2.1 and 4.2 V at current density of 15, 75 and 150 mA g^{-1} respectively on an Arbin BT2000 battery tester.

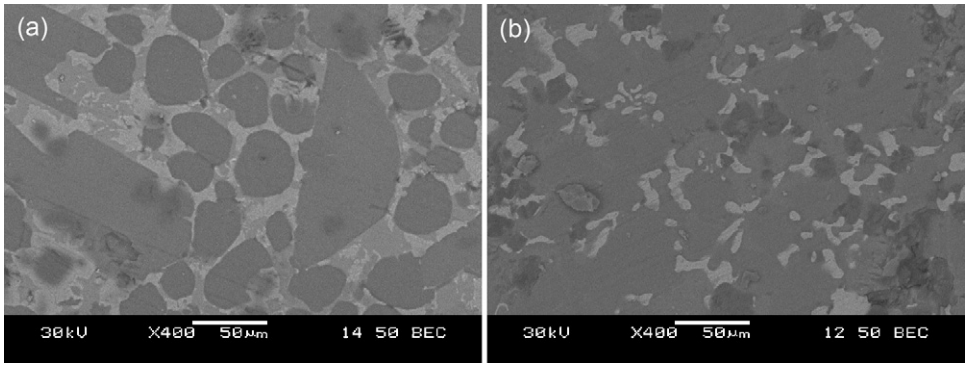

Fig. 1. Backscatter electron images of ground section of (a) as-received slag and (b) reduced slag.

3. Results and discussion

3.1. Selective recovery of Fe, Mn, V and Cr from steel slag

The selective carbothermic process is employed in the recovery of Fe, Mn, V and Cr from steel slag in order to exclude silicon in the meantime. In theory, the carbothermic reduction of oxides of Fe, P, Cr, Mn, and V in the slag could proceed at a certain temperature, whereas that of the other oxides (such as oxide of Si, Ti, Al, Mg, and Ca) needs higher temperature at the same partial pressure of oxygen. In present study, the temperature employed in the carbothermic process was thus selected as 1400 °C to prevent the extraction of Si from the slag along with Fe.

Backscatter electron images of ground section of the as-received slag and reduced slag are given in Fig. 1. As shown in Fig. 1a, the microstructure of the slag is usually identified as three distinct phases [26]: dicalcium silicate phase (the dark gray phase in Fig. 1a), RO phase (the off-white phase, including metal oxides such as FeO, MgO and MnO) and calcium aluminoferrite phase (the light gray phase). The major metals in the slag are usually Fe, Mn, V and Cr. Fe mainly consists in RO phase and calcium aluminoferrite phase in the form of iron oxide and Fe-bearing minerals along with manganic oxides. V and Cr chiefly consist in calcium aluminoferrite phase also. As a dominant phase of steel slag, the dicalcium silicate phase seldom contains other elements besides Ca, Si, O, and P. To sum up, Mn, V, and Cr always exists in the Fe-concentrating phases of the slag. Such an elemental distribution is of benefit to the diffusion of Mn, V, and Cr into Fe to form a ferroalloy in selective carbothermic process.

Fig. 1b shows the microstructure of the steel slag treated by carbothermic process at 1400 °C for 2 h. The white phase presents the ferroalloy precipitated in RO phase and calcium aluminoferrite phase. The mean dimension of the ferroalloy phases is of about 10 μm, which basically satisfies the need of the separation of the ferroalloy from tailing. The ferroalloy separated from tailing by magnetic separation is then oxidized to the R-oxides.

As shown in Table 1, the chemical composition of the slag indicates the presence of 23.26 wt.% TFe (total Fe in the slag), 2.52 wt.% MnO, 2.07 wt.% P_2O_5, 0.86 wt.% V_2O_5, and 0.53 wt.% Cr_2O_3 and other oxides relating to Ca, Mg, Si, Al, Ti, and so on. The major component of recovered R-oxides is ferric oxides (Fe_2O_3, 88.82 wt.%), and the oxides in small amounts are P_2O_5, MnO, V_2O_5, and Cr_2O_3 with contents of 3.14, 4.64, 1.12 and 1.40 wt.%, respectively. The sum of CaO, SiO_2, MgO, $A1_2O_3$, TiO_2, and NiO existing in the R-oxides is merely 0.62%, which can be regarded as negligible impurities.

Table 2 lists the molar ratio of Fe and other elements in the as-received slag and recovered R-oxides, respectively. About 80 wt.% of Fe in steel slag was recovered through carbothermic process. Regarding the microelements in slag, about half of Mn, P, V, and Cr in the slag was also recovered along with Fe because of their high solid solubilities in ferrite. On the other hand, the major elements of the slag, Ca, Si, and Mg, are hardly reduced by C in experimental conditions and seldom present in the R-oxides. As a result, all components of obtained R-oxides are useful to synthesis of M-$LiFePO_4$/C except for a small quantity of impurities, and the molar ratio of Fe to Mn, V, and Cr in R-oxides is satisfactory. The selectivity of recovery of the valuable elements from the slag is achieved.

Table 2
The molar ratio of Fe and other elements in steel slag and recovered R-oxides.

Sample	As-received steel slag	Recovered R-oxides
Fe	100	100
Ca	214.02	0.13
Si	79.13	0.32
Mg	53.09	0.32
Mn	8.55	5.89
P	17.55	3.98
Al	7.22	0.23
V	2.28	1.11
Cr	1.68	1.66
Ti	1.26	0.02
Ni	0.32	0.05

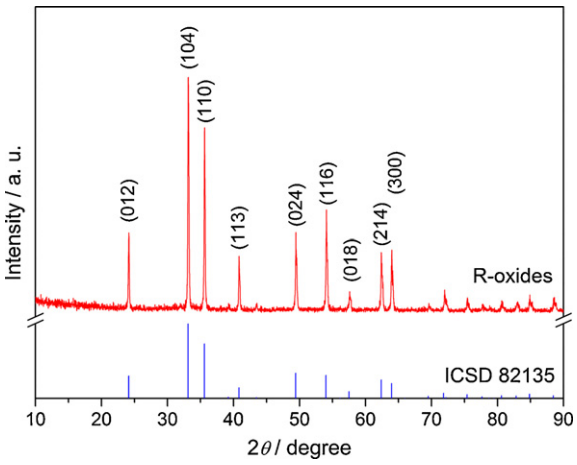

Fig. 2. The X-ray diffraction pattern of the R-oxides.

Fig. 2 gives the X-ray diffraction pattern of the R-oxides powders. The characteristics of typical peaks for the R-oxides are quite consistent with those given by ICSD 82135 published in PDF2004 database. Neither peak shifts nor distinct new peaks were detected on the measured XRD patterns. The results indicate that the R-oxides approximately exhibits the crystal structure of Fe_2O_3, and Mn, P, V, and Cr may be doped into crystal lattice of Fe_2O_3 to form the multi-doped ferric oxides.

3.2. Synthesis and characterizations of M-$LiFePO_4$/C and U-$LiFePO_4$/C

In order to evaluate the electrochemical properties of M-$LiFePO_4$/C synthesized from steel slag, we prepared an U-$LiFePO_4$/C sample by using chemical reagents as source materials under the same conditions for comparison. SEM images of M-$LiFePO_4$/C and U-$LiFePO_4$/C powders are shown in Fig. 3. As shown, the microstructure of M-$LiFePO_4$/C is very similar to that of U-$LiFePO_4$/C. Fine particles in the size of 200–500 nm can be observed in despite of severe particle aggregation occurred in both samples. This indicates that using steel slag as raw material does not influence the microstructure of M-$LiFePO_4$/C markedly.

Fig. 4 shows the elemental mapping (Fe, P, Mn, V, and Cr) of prepared M-$LiFePO_4$. The highlight areas in SE image are bulges of agglomerated particles in the field of view. The distribution areas for elements (Fe, P, Mn, V and Cr) are homogeneous. It demonstrates that the dopants deriving from steel slag had achieved homogeneous solid solution with $LiFePO_4$. Although the distribution of doping elements in particles is homogeneous as expected, further analysis by X-ray diffraction (XRD) is still required to verify if the doping elements are incorporated in the lithium iron phosphate crystal.

Fig. 5 gives the Rietveld refinement of X-ray powder diffraction pattern for M-$LiFePO_4$/C. The XRD pattern of U-$LiFePO_4$/C is inset in the top right corner of Fig. 5 for comparison. The XRD pattern for M-$LiFePO_4$/C is refined without considering the trace elements (Al, Ti, Ni, Si, Ca, etc.) from the R-oxides, and the crystal parameters are summarized in Table 3.

The X-ray diffraction profile measured for M-$LiFePO_4$/C was refined by Rietveld analysis considering Mn, V, and Cr as doping

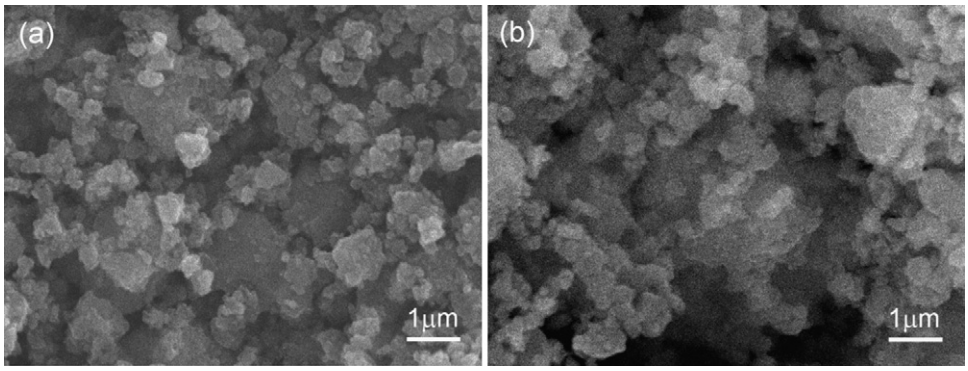

Fig. 3. SEM images of (a) U-$LiFePO_4$/C and (b) M-$LiFePO_4$/C powders.

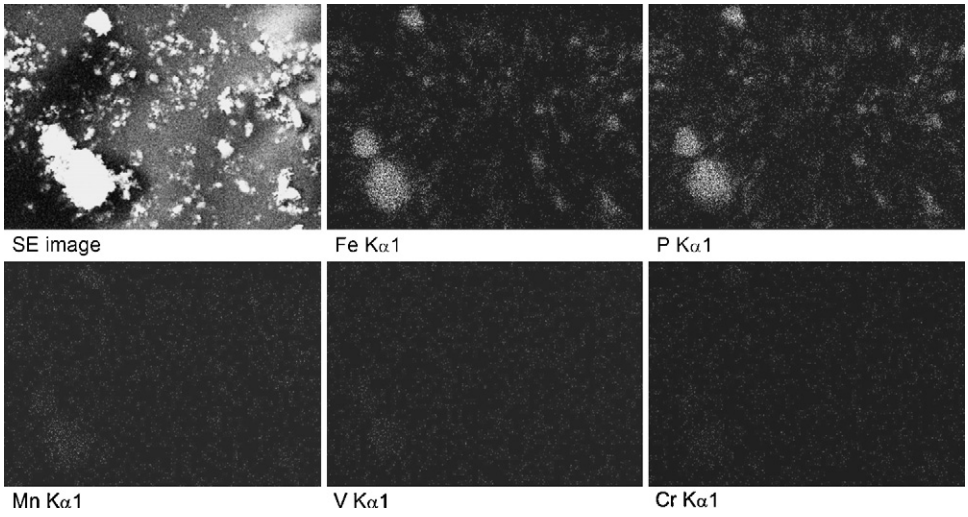

Fig. 4. Elemental mapping of M-$LiFePO_4$ powder prepared from steel slag.

elements. For synthesis of M-$LiFePO_4$/C in this work, what sites in the crystal lattice of olivine $LiFePO_4$ for Mn, V, and Cr to occupy is the chief consideration. Many works have reported that Mn [14–17] and V [18,19] are primarily located on the Fe site. However, the preferred site for Cr is still an open question. According to the reports in previous literature, we find that doping of Cr on Li sites [20–22] and on Fe sites [23,24] could all achieve good electrochemical properties. It seems that Mn, V, and Cr can all be located on the Fe site. In the present work, we prepared the M-$LiFePO_4$/C using Mn + V + Cr recovered from steel slag to substitute the equivalent amount of Fe. The Rietveld refinement patterns of the XRD profile demonstrate that pure olivine $LiFePO_4$ phase was obtained (Fig. 5).

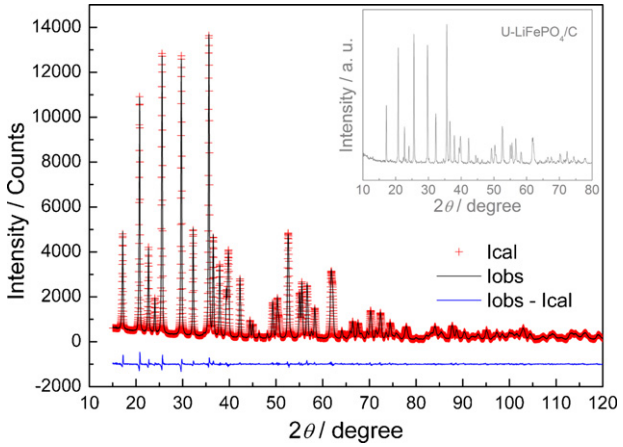

Fig. 5. Rietveld profile refinement of XRD patterns for M-$LiFePO_4$/C powders (R_{wp} = 0.0876, R_p = 0.0688). Inset: the XRD pattern of U-$LiFePO_4$/C.

As shown in Fig. 5, the Rietveld refinement patterns of the XRD profile for M-$LiFePO_4$/C indicate the good crystallinity of samples. All peaks can be indexed based on the orthorhombic $LiFePO_4$ crystallizing in the space group *Pnma*. No impurity phase was identified in observed pattern. The observed pattern and calculated pattern match well, and the agreement factors (R_{wp}, weighted pattern factor; R_p, pattern factor) are satisfactory (R_{wp} = 0.0876, R_p = 0.0688). Structural parameters listed in Table 3 indicate that the fitting result is very good when Mn, Cr, and V are considered all on Fe site. The unit cell parameters of M-$LiFePO_4$/C obtained by Rietveld refinement are a = 10.3203(2) Å, b = 6.0050(3) Å, and c = 4.6907(9) Å, which are in a good agreement with the standard data (a = 10.332 Å, b = 6.010 Å, and c = 4.692 Å) given by ICSD 72545. Results of Rietveld

Table 3
Structural parameters obtained by the Rietveld refinement of XRD pattern recorded for M-$LiFePO_4$/C. Space group: *Pnma*. Lattice constant: (Å): a = 10.3203(2), b = 6.0050(3), c = 4.6907(9); Unit cell volume (Å^3): 290.7062(3).

Atom	Site	Occupancy	Atom position		
		N	*X*	*Y*	*Z*
Li	4a	1	0	0	0
(Fe + Mn + Cr + V)	4c	1	0.2831(3)	0.2504(2)	0.9746(1)
P	4c	1	0.0949(8)	0.2498(8)	0.4184(6)
O1	4c	1	0.0963	0.2504(8)	0.7537(5)
O2	4c	1	0.4574(2)	0.2504(9)	0.2095(9)
O3	8d	1	0.1665(6)	0.0440(4)	0.2799(6)

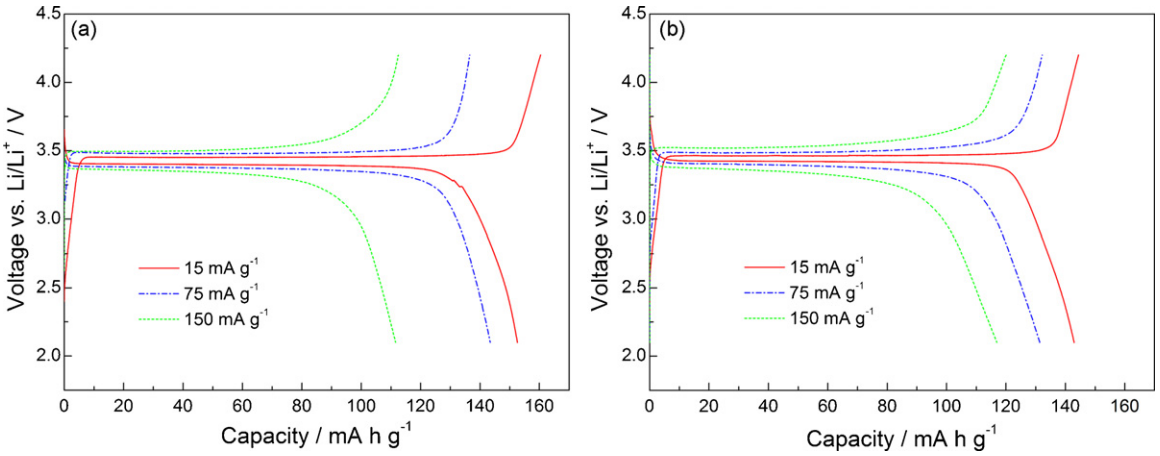

Fig. 6. The initial charge/discharge curves of (a) U-LiFePO$_4$/C and (b) M-LiFePO$_4$/C at different current densities in the voltage range of 2.1–4.2 V at room temperature.

refinement confirm that the doping elements have been incorporated in the lithium iron phosphate crystal.

The inset in Fig. 5 shows the XRD pattern for U-LiFePO$_4$/C sample prepared from chemical reagents under the same conditions. The positions and profiles of typical peaks exhibit a good consistency with those of M-LiFePO$_4$/C sample prepared from steel slag. The unit cell parameters calculated by the XRD data of U-LiFePO$_4$/C are $a = 10.3325(3)$ Å, $b = 6.0057(8)$ Å, and $c = 4.6932(4)$ Å. The values are very close to those of M-LiFePO$_4$/C sample prepared from steel slag, and also in a good agreement with the standard data given by ICSD 72545. The results demonstrate that using steel slag as source materials of Fe and multi-doping elements does not remarkably distort the crystal structure of LiFePO$_4$.

3.3. *Electrochemical properties*

Electrochemical measurements have been performed for M-LiFePO$_4$/C and U-LiFePO$_4$/C samples. The EDS analysis for M-LiFePO$_4$/C indicates the presence of a certain amount of Mn, V, and Cr in the sample, respectively. The multiple dopants and carbon are considered as the indiscerptible part for building up whole active materials, and those contents are not deducted in calculating the capacities of the active material samples.

Fig. 6 shows the voltage profiles of initial charge/discharge with different current densities for U-LiFePO$_4$/C and M-LiFePO$_4$/C cathodes in the voltage range of 2.1–4.2 V at room temperature. Fig. 7 represents their cycling performance. The results indicate that both the voltage profiles of U-LiFePO$_4$/C and M-LiFePO$_4$/C exhibit good shapes with very plat plateaus around 3.4 V at different current densities. The initial discharge curve of U-LiFePO$_4$/C shows a capacity of 155 mAh g^{-1} at a low current density of 15 mA g^{-1}, which is close to the theoretical capacity of LiFePO$_4$ (170 mAh g^{-1}). However, the discharge capacity of U-LiFePO$_4$/C decreases rapidly to 142 and 112 mAh g^{-1} with increasing of the charge/discharge current density to 75 and 150 mA g^{-1}, respectively. In contrast, the discharge capacities of M-LiFePO$_4$/C show 143 mAh g^{-1} at a current density of 15 mA g^{-1}, 131 mAh g^{-1} at 75 mA g^{-1}, and 117 mAh g^{-1} at 150 mA g^{-1}, respectively. For cycling performance shown in Fig. 7, both U-LiFePO$_4$/C and M-LiFePO$_4$/C present excellent capacity retention at current density of 75 and 150 mA g^{-1}. The mean capacity of U-LiFePO$_4$/C with a fixed current density decreases by 10% and 20% when the current density increased from 15 to 75 mA g^{-1} and from 75 to 150 mA g^{-1}, but in contrast that of M-LiFePO$_4$/C decreased merely by 8% and 12%, respectively. The results suggest that the M-LiFePO$_4$/C prepared from steel slag exhibits a better rate performance than U-LiFePO$_4$/C.

Compared to a quick decrease in discharge capacity for U-LiFePO$_4$/C with increasing of the current density, the improvement on the capacity decrease for M-LiFePO$_4$/C should be ascribed to the multi-doping of Mn, V, and Cr into LiFePO$_4$. The multi-doping induces an increase of Li^+ ion mobility obtained by the substitution of doping cations for Fe^{2+} [17], and facilitates the phase transformation between LiFePO$_4$ and FePO$_4$ during cycling and thus improves the rate performances of LiFePO$_4$ [23]. Furthermore, the investigation based on the first-principle calculation reported that the enhancement of electronic conductivity could be achieved by replacing Fe ions with Mn cations [27].

Cyclic voltammogram (CV) profiles of the U-LiFePO$_4$/C and M-LiFePO$_4$/C, collected at a scanning rate of 0.1 mV s^{-1} are shown in Fig. 8. A couple of very well defined redox peaks could be seen in CV profiles of both U-LiFePO$_4$/C and M-LiFePO$_4$/C. The redox peaks of the U-LiFePO$_4$/C at 3.640/3.250 V with a redox potential separation of 0.39 V could be attributed to the Fe^{3+}/Fe^{2+} redox couple transformation, accompanied by lithium ion insertion/extraction into and out of the electrode. The Fe^{3+}/Fe^{2+} redox peaks of M-LiFePO$_4$/C were located at 3.575/3.325 V, with a redox potential separation of 0.25 V. The obvious decrease in the redox potential separation also implies that the electrode reactivity is improved by the multi-doping behaviors.

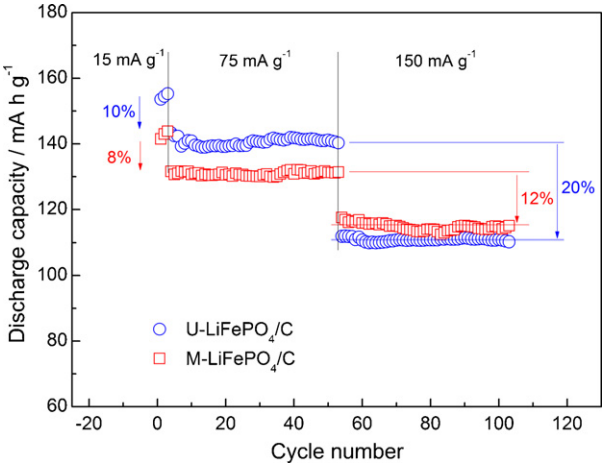

Fig. 7. Cycling performance of U-LiFePO$_4$/C and M-LiFePO$_4$/C at different electric current densities. The cell cycled 3 times at 15 mA g^{-1}, then cycled 50 times at 75 mA g^{-1} and 150 mA/g in turn.

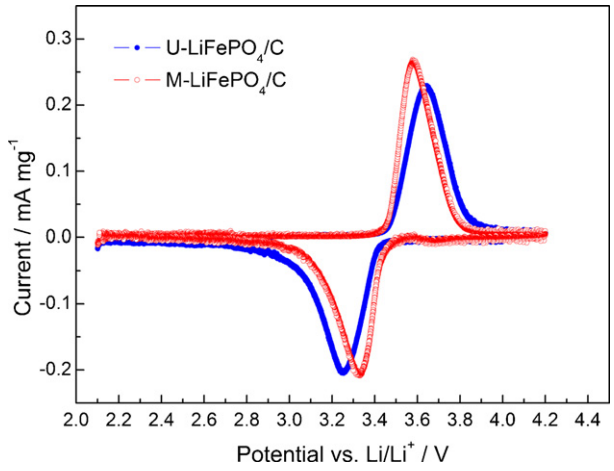

Fig. 8. Cyclic voltammograms of U-$LiFePO_4$/C and M-$LiFePO_4$/C cathodes at a scanning rate of 0.1 mV s^{-1}.

4. Conclusions

The ferroalloy with suitable content of Fe, Mn, V, and Cr was recovered from steel slag by selective carbothermic method, and successfully used as source materials of Fe and multi-dopants (Mn, V, and Cr) in synthesis of the M-$LiFePO_4$/C powders. The Rietveld refinement for XRD pattern of the M-$LiFePO_4$/C confirms that Mn, V, and Cr atoms all occupy Fe site, and does not introduce any impurity phase and remarkable lattice distortions. Elemental mapping image confirms that the elements (Fe, P, Mn, V, and Cr) distribute homogeneously in particles of the multi-doped $LiFePO_4$/C. Electrochemical tests shows that the M-$LiFePO_4$/C prepared from the slag delivers a capacity of 143, 131, and 117 mAh g^{-1} at a current density of 15, 75, and 150 mA g^{-1}, respectively, and exhibits very good capacity retention. Compared to U-$LiFePO_4$/C prepared only from chemical reagents, the M-$LiFePO_4$/C sample prepared from the slag exhibits a better rate performance due to the improvement of the electrode reactivity by multi-doping, particularly at higher current rates. The results demonstrate that a feasible route to utilize the steel slag in a high added value manner has been offered.

Acknowledgements

This work was financially supported by Anhui Education Department of China (No. KJ2008A038, KJ2009A69) and the International Cooperation Project from Anhui Science & Technology Department of China (No. 09080703019). The experimental support from the Innovation Group of Anhui University of Technology was also acknowledged.

References

[1] S. Porisiensi, Iron Steel Technol. 1 (2004) 63–66.
[2] F. Memoli, C. Mapelli, M. Guzzon, Iron Steel Technol. 4 (2007) 68–76.
[3] Y. Xue, S. Wu, H. Hou, J. Zha, J. Hazard. Mater. 138 (2006) 261–268.
[4] P. Chaurand, J. Rose, V. Briois, L. Olivi, J.L. Hazemann, O. Proux, J. Domas, J.Y. Bottero, J. Hazard. Mater. B139 (2007) 537–542.
[5] D. Adolfsson, N. Menad, E. Viggh, B. Björkman, Adv. Cement Res. 19 (2007) 133–138.
[6] A. Oner, S. Akyuz, Cement Concrete Comp. 29 (2007) 505–514.
[7] P.E. Tsakiridis, G.D. Papadimitriou, S. Tsivilis, C. Koroneos, J. Hazard. Mater. 152 (2008) 805–811.
[8] F.A. Lopez, N. Balcazar, A. Formoso, M. Pinto, M. Rodrıguez, Waste Manage. Res. 13 (1996) 555–568.
[9] X. Wang, Q.S. Cai, Pedosphere 16 (2006) 519–524.
[10] H.T. Shen, E. Forssberg, Waste Manage. 23 (2003) 933–949.
[11] K. Morita, M.X. Guo, N. Oka, N. Sano, J. Mater. Cycles Waste Manage. 4 (2002) 93–101.
[12] S.M. Jung, Y.J. Do, J.H. Choi, Steel Res. Int. 77 (2006) 305–311.
[13] S.M. Jung, Y.J. Do, Steel Res. Int. 77 (2006) 312–316.
[14] M. Bini, M.C. Mozzati, P. Galinetto, D. Capsoni, S. Ferrari, M.S. Grandi, V. Massarotti, J. Solid State Chem. 182 (2009) 1972–1981.
[15] J. Molenda, W. Ojczyk, J. Marzec, J. Power Sources 174 (2007) 689–694.
[16] C.M. Burba, R. Frech, J. Power Sources 172 (2007) 870–876.
[17] K.T. Lee, K.S. Lee, J. Power Sources 189 (2009) 435–439.
[18] C.S. Sun, Z. Zhou, Z.G. Xu, D.G. Wang, J.P. Wei, X.K. Bian, J. Yan, J. Power Sources 193 (2009) 841–845.
[19] M.R. Yang, W.H. Ke, J. Electrochem. Soc. 155 (2008) A729–A732.
[20] S.Y. Chung, J.T. Bloking, Y.M. Chiang, Nat. Mater. 1 (2002) 123–128.
[21] J.R. Ying, M. Lei, C.Y. Jiang, C.R. Wan, X.M. He, J.J. Li, L. Wang, J.G. Ren, J. Power Sources 158 (2006) 543–549.
[22] M. Wagemaker, B.L. Ellis, D. Lützenkirchen-Hecht, F.M. Mulder, L.F. Nazar, Chem. Mater. 20 (2008) 6313–6315.
[23] H.C. Shin, S.B. Park, H. Jang, K.Y. Chung, W.I. Cho, C.S. Kim, B.W. Cho, Rate performance and structural change of Cr-doped $LiFePO_4$/C during cycling, Electrochim. Acta 53 (2008) 7946–7951.
[24] V. Lemos, S. Guerini, J.M. Filho, S.M. Lala, L.A. Montoro, J.M. Rosolen, Solid State Ionics 177 (2006) 1021–1025.
[25] R.K.B. Gover, A. Bryan, P. Burns, J. Barker, Solid State Ionics 177 (2006) 1495–1500.
[26] G.H. Hou, W.F. Li, W. Guo, J.H. Chen, J.H. Luo, J.G. Wang, J. Chin. Ceram. Soc. 36 (2008) 436–443.
[27] J. Xu, G. Chen, Physica B, doi:10.1016/j.physb.2009.05.035.